Journal of large-scale research facilities

Journal of large-scale research facilities, 4, A127 (2018) http://dx.doi.org/10.17815/jlsrf-4-77

Published: 17.01.2018

The UE46 PGM-1 beamline at BESSY II

Helmholtz-Zentrum Berlin für Materialien und Energie [*]

Instrument Scientists:
- Dr. Eugen Weschke, Abteilung Quantenphänomene in neuen Materialien (EM-AQM) Helmholtz -Zentrum Berlin für Materialien und Energie, phone: +49 30 8062-13409, email: eugen.weschke@helmholtz-berlin.de
- Dr. Enrico Schierle, Abteilung Quantenphänomene in neuen Materialien (EM-AQM) Helmholtz -Zentrum Berlin für Materialien und Energie, phone: +49 30 8062-15760, email: enrico.schierle@helmholtz-berlin.de

Abstract: The UE46 PGM-1 undulator beamline at the BESSY II storage ring provides soft x-rays of tunable polarization, linear and circular. With two permanent endstations, a versatile XUV diffractometer and a 7-Tesla High-Field diffractometer, the setup is dedicated to both, resonant spectroscopy and scattering/diffraction.

1 Introduction

UE46 PGM-1 is one of two beamlines sharing the elliptical undulator UE46 at BESSY II, Berlin. Photon energies available at the beamline range from 120 eV to 2000 eV. The polarization is tunable, providing various linear and circular states. The beamline is of plane-grating design (Follath & Senf, 1997) with a fixed-focus geometry, as shown in Figure 1 (Englisch et al., 2001). The last mirror chamber of the beamline hosts two mirrors that can be switched to provide either a focused or a collimated beam at the experiment (cases A and B in Figure 1). As typical for an undulator beamline, high photon flux of the order of 1012 photons/second is provided (Englisch et al., 2001).

[*] **Cite article as:** Helmholtz-Zentrum Berlin für Materialien und Energie. (2018). The UE46 PGM-1 beamline at BESSY II . *Journal of large-scale research facilities, 4*, A127. http://dx.doi.org/10.17815/jlsrf-4-77

[H]

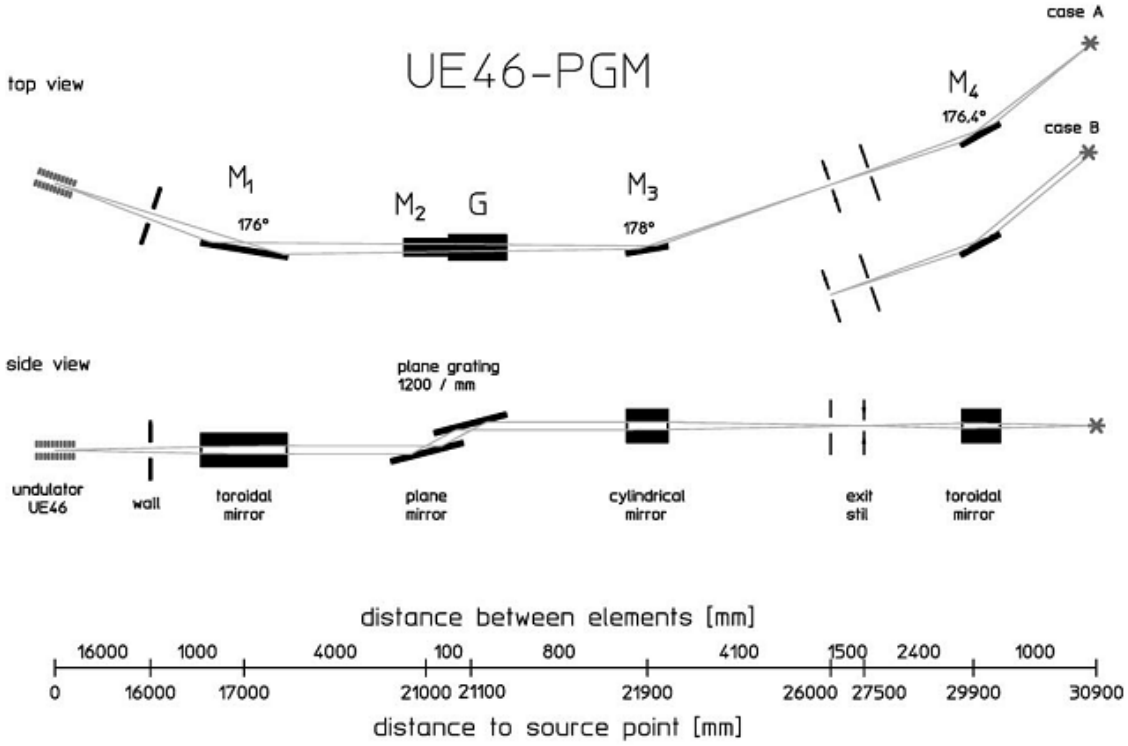

Figure 1: Optical layout of the beamline UE46 PGM-1 (Reprinted from Nuclear Instruments and Methods in Physics Research Section A: Accelerators, Spectrometers, Detectors and Associated Equipment, Volumes 467–468, Part 1, Englisch et al. (2001): The elliptical undulator UE46 and its monochromator beam-line for structural research on nanomagnets at BESSY-II page 544, Copyright (2017) with permission from Elsevier).

Techniques employed at UE46 PGM-1 include polarization-dependent X-ray absorption (XAS), such as X-ray magnetic circular dichroism (XMCD) or X-ray magnetic circular dichroism (XMLD), and resonant soft X-ray scattering (RSXS) experiments, covering a wide range of materials and scientific questions. Continuous-mode scanning of the photon energy is implemented at the beamline, pairs of XMCD spectra can be recorded with very high quality within 10 minutes and less. Depending on the sample, noise-to-signal ratios as low as 10-4 have been achieved by measurement of the total electron yield (TEY). The beamline features two permanent endstations, the XUV Diffractometer, an instrument dedicated to high-performance RSXS studies, and the High-Field Diffractometer for RSXS and XAS studies in magnetic fields up to 7 Tesla. Both endstations are placed along the beam direction and are connected by a vacuum tube. Beamline and instruments can be separated by ultrathin polyimide windows, which are transparent in the soft x-ray region. Together with swift switching between focused and collimated beam, this allows for both instruments being used within the same beam time. A photograph of the setup is shown in Figure 2. Beamline and endstations are controlled by the SPEC program from Certified Scientific Software. The instrumentation is operated by the Department Quantum Phenomena in Novel Materials at HZB.

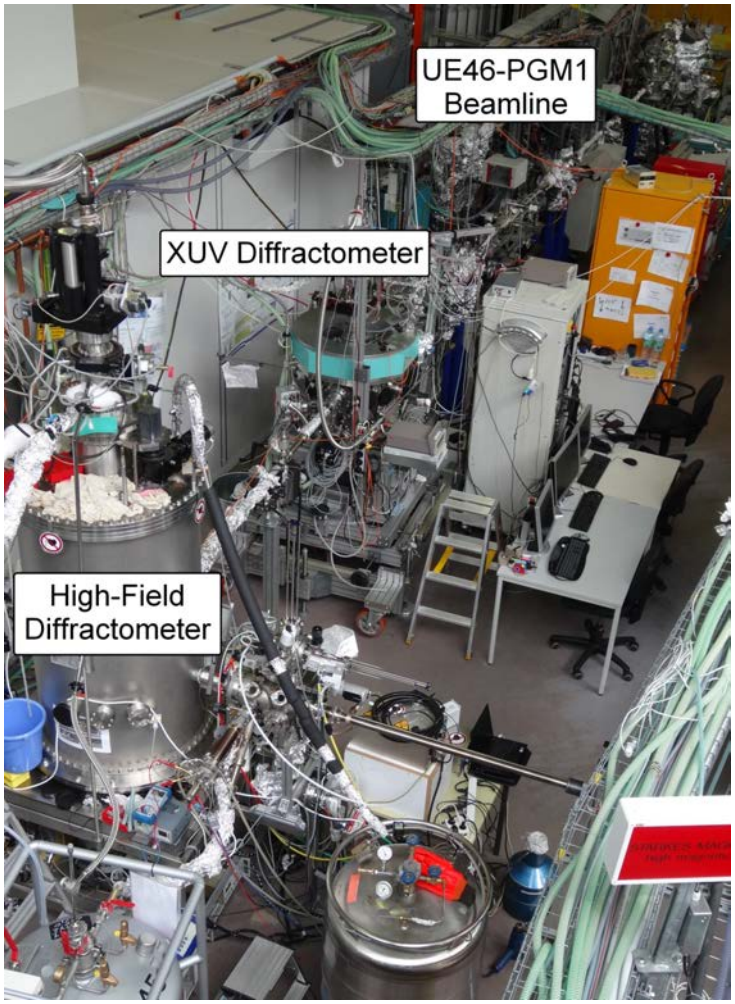

Figure 2: Overview of beamline UE46 PGM-1 with the two endstations.

2 Experimental Endstations

2.1 XUV Diffractometer

The XUV Diffractometer is a dedicated endstation to explore electronic ordering phenomena, like magnetic, charge and orbital ordering by resonant soft x-ray scattering (RSXS) experiments. This versatile endstation is a UHV-compatible two-circle diffractometer operating in horizontal scattering geometry with the sample and detector rotations driven from outside the vacuum by two Huber circles with highest accuracy and stability. Together with very stable X-ray beam conditions, this allows to perform high quality diffraction experiments even from tiny crystals (< 100 μm x 100 μm) over a large angular range, as well as measurements of specular reflectivity with very high precision.
The standard setup features a sample holder directly attached to a liquid He-flow-cryostat, providing sample temperatures below 4 K. Azimuthal rotation in situ is provided for azimuth-dependent measurements even at these low temperatures (Leininger et al., 2010; Princep et al., 2012).
Photons are detected by an AXUV100-type photodiode with a set of changeable slits in front for adapting the resolution. The detector can be scanned in the direction perpendicular to the scattering plane. This allows to compensate possible Chi-misalignment of the sample without compromising with respect to the lowest sample temperatures. The experimental setup allows for XAS masurements by parallel monitoring of the sample drain current (TEY measurements) as well as for FY measurements. Beyond the standard setup of sample mounting, the XUV diffractometer is highly flexible and can adapt to special sample mounting. The instrument usually runs with a vacuum in the range of 10-9 mbar, but UHV conditions can be achieved, if required. More details about the XUV diffractometer and related RSXS experiments can be found in (Fink et al., 2013).

2.2 High-Field Diffractometer

The High-Field Diffractometer is an endstation for both XAS and RSXS in magnetic fields up to 7 Tesla, and temperatures down to 4 K. This combination of high magnetic fields and low temperatures renders the setup ideal for studying weakly coupled magnetic systems like diluted magnets or single molecular magnets. The unique feature of this endstation is a superconducting coil that can be rotated in vacuum independently from the sample. The station is therefore perfectly suited for XMCD and XMLD experiments in various geometries. The absorption signal is typically measured in TEY mode via the sample drain current. Employing continuous-mode photon energy scans, pairs of energy-dependent absorption scans with opposite light helicities can be recorded with very high quality within 10 minutes or even less. Depending on the sample, noise-to-signal ratios as low as 10^{-4} have been achieved. A rotatable photon detector permits dichroic experiments also in specular reflectivity, which is less surface sensitive than TEY-mode experiments, and which can be tuned to increase the sensitivity towards tiny magnetizations at interfaces.
The same detector permits RSXS experiments with a horizontal scattering plane as in case of the XUV Diffractometer in order to study the evolution of electronic ordering phenomena, like charge and orbital ordering in high magnetic fields. While the previously described XUV Diffractometer allows for scattering angles in the full range from zero to approximately 180 degrees, this is not possible due to geometrical constraints by the magnet. Nevertheless, the rotatable magnet with its split-coil design allows for various geometries to be chosen for scattering experiments. The accessible scattering angles and respective magnetic field directions can be inferred from the schematic drawing in Figure 4. Experience from previous experiments certifies many relevant geometries to be accessible for the study of complex materials. A particular strength of the setup at the UE46 PGM-1 beamline is the possible use of both endstations for one experiment, permitting convenient studies in the XUV diffractometer before moving on to high-field research.
Samples can be fast transferred from outside vacuum through a three-stage load lock system to a sample holder directly attached to a liquid He flow cryostat that provides base temperatures of the order of

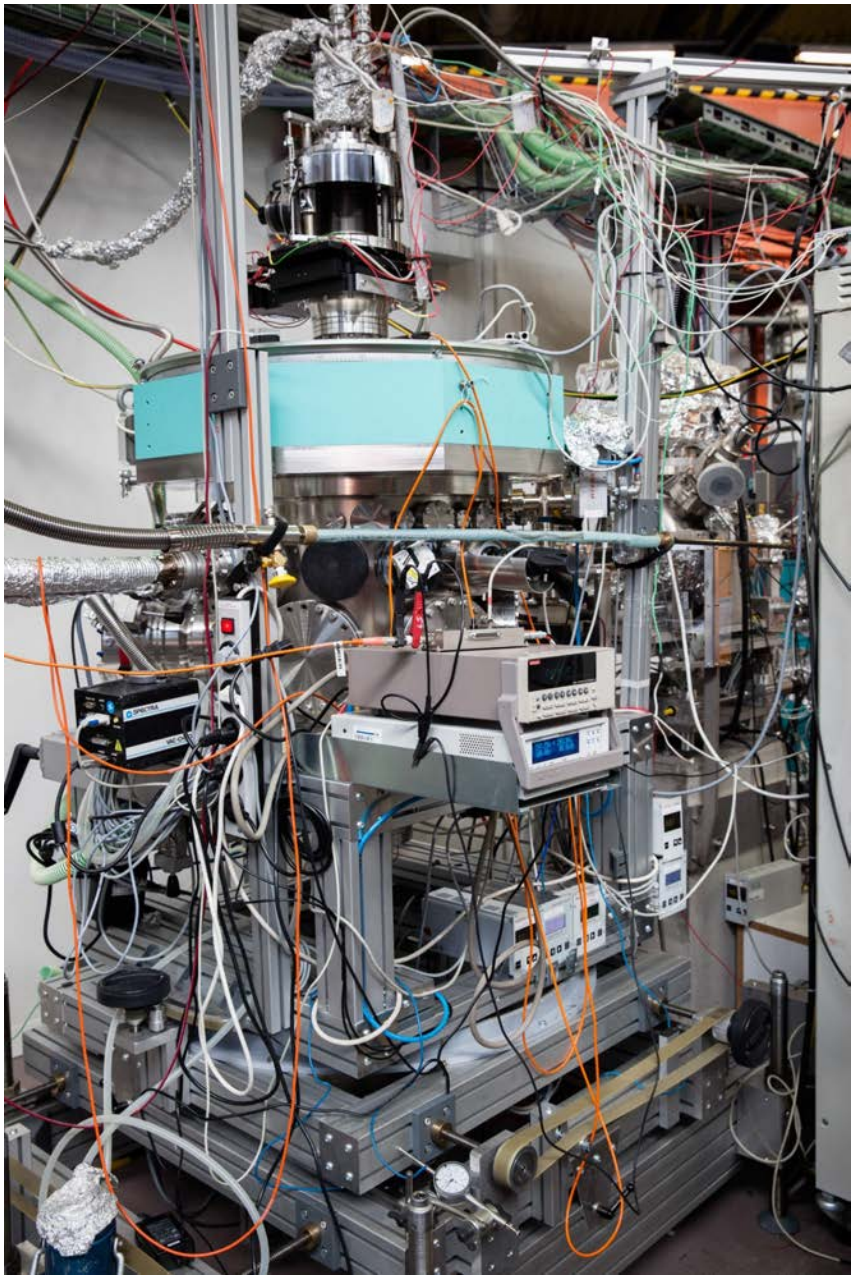

Figure 3: View of the XUV Diffractometer with the detector circle painted in the typical Huber color.

4 K. The last chamber of the load-lock system provides flexibility with respect to sample treatment before the measurement. While this is not a fully equipped surface-analysis UHVchamber, a range of surface preparation tools can be installed, providing evaporation in situ, ion etching, sample annealing, cleavage of crystals. Even user instrumentation can be attached to the load-lock chamber to some extent.

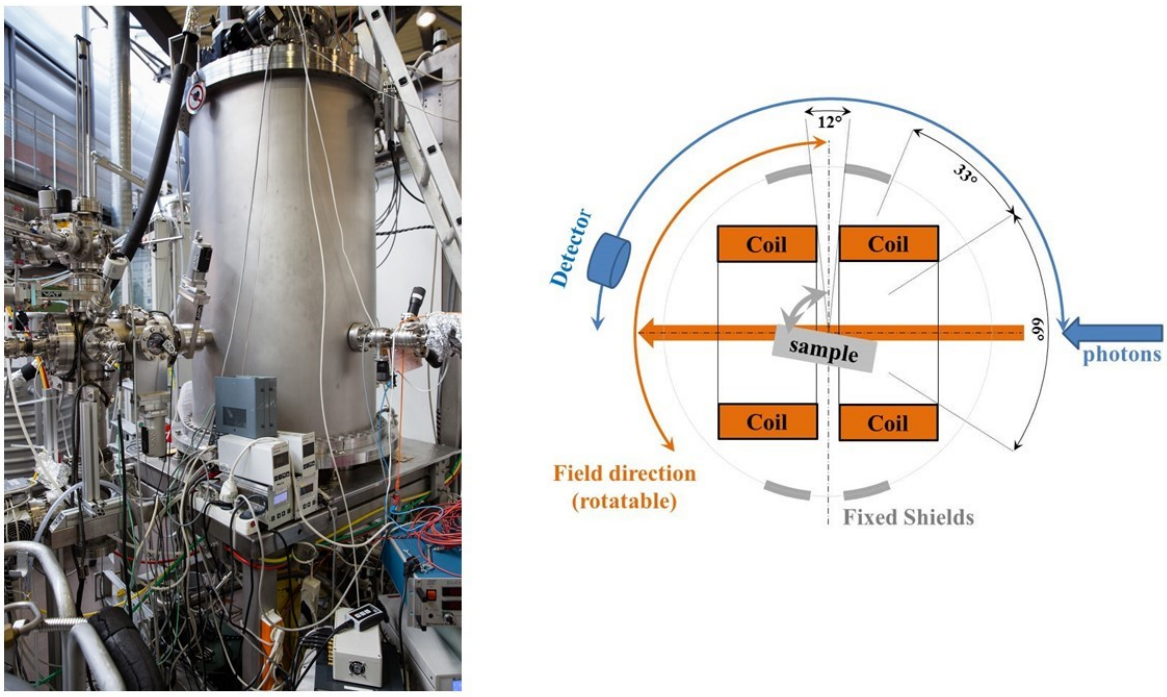

Figure 4: View of the High-Field Diffractometer (left) and schematic representation of the scattering plane (right).

3 Applications

The UE46 PGM-1 beamline and its two endstations have been used in various studies, where both XAS and RSXS were widely employed. Topics are ranging from magnetic coupling in single-molecule magnets at surfaces to subtle ordering phenomena in high-Tc superconducting cuprates. An account of the latter technique applied to complex electronic superstructures has originated from studies at the beamline and is given in (Fink et al., 2013).
In order to illustrate the scope of science and materials associated with the instrumentation, we list here a few topics that concerned studies at UE46 PGM-1

- Charge order of high-Tc Superconductors (Blanco-Canosa et al., 2013; Comin et al., 2014; da Silva Neto et al., 2014; Fink et al., 2009; Ghiringhelli et al., 2012)
- Coupling of electronic / lattice degrees of freedom in multiferroic materials (Glavic et al., 2013; Partzsch et al., 2011; Schierle et al., 2010; Schmitz-Antoniak et al., 2013; Skaugen et al., 2015)
- Microcrystals of novel materials (Leininger et al., 2011; Matsuda et al., 2015)
- Interfacial electronic properties in heterostructures (Frano et al., 2013; Wadati et al., 2009)
- Element-specific magnetic hysteresis loops (Radu et al., 2012)
- Single molecular magnets (Bernien et al., 2015; Hermanns et al., 2013)
- Electronic depth profiles

- Electronic ground states and phase transitions in correlated materials (Schmitz et al., 2014; Strigari et al., 2013; Willers et al., 2012, 2011)
- Magnetic clusters in carbon nanotubes (Shiozawa et al., 2015)
- Nanoparticles for medical applications (Graf et al., 2015)
- Magnetic semiconductors (Khalid et al., 2014)

4 Technical Specifications

4.1 4.1 Source

The insertion device is the elliptical undulator UE46 with the following parameters:

Type	APPLE2
Location	L10
Period length	46.3 mm
Periods/Pols	70 n
Minimal energy at 1,7 GeV	109 eV
Minimal gap	15.6 mm
Polarisation	linear variable 0° ... +90° elliptical, circular

Table 1: Parameters of insertion device UE46.

4.2 Beamline

See also: UE46_PGM-1 (www.helmholtz-berlin.de)

The UE46 PGM-1 beamline has the following characteristics:

Location	11.22
Source	UE46
Monochromator	PGM
Energy range	120 - 2000 eV
Energy resolution	10,000
Flux	10^{12}
Polarisation	• Linear any angle (with restrictions) • Circular
Divergence horizontal	1 mrad
Divergence vertical	1 mrad
Focus size (hor. x vert.)	• Focussed beam: typically 100 μm x 50 μm ultimate: 40 μm x 10 μm • Collimated beam: $\leq$ 1.7 mm x 1.5 mm (depending on apertures)
Distance focus/last valve	565 mm
Height focus/floor level	1417 mm
Free photon beam available	Only under special conditions (please contact the beamline scientist before application)
Fixed end station	Yes
Software	SPEC

Table 2: Technical data of Beamline UE46 PGM-1.

4.3 XUV Diffractometer

See also: XUV Diffractometer (www.helmholtz-berlin.de)

Experiment in vacuum	Yes, down to UHV conditions
Temperature range	3.8 - 320 K (for T = 3.0 K contact Station Managers)
Detector	AXUV100 type photodiode
Scattering geometry	Horizontal
Angular range	Unlimited (360 deg.)
Maximum sample size	5 mm x 5 mm
Azimuthal sample rotation	Yes
Software	SPEC

Table 3: Technical data of the XUV Diffractometer at UE46 PGM-1.

4.4 High-Field Diffractometer

See also: High-Field Diffractometer (www.helmholtz-berlin.de)

Experiment in vacuum	Yes
Temperature range	4 - 350 K
XAS measurement scheme	Total electron yield (drain)
Detector	AXUV100 type photodiode
Magnetic field	Standard: 6 Tesla (for fields up to 7 Tesla contact Station Managers)
Magnetic field geometry	Horizontal, rotatable (90 deg.) with respect to sample
Scattering geometry	Horizontal
Sample rotation	0 deg. to 90 deg. with respect to the photon beam
Scattering angles	Limited, depending on orientation of the magnet (cf. Figure 4)
Software	SPEC

Table 4: Technical data of the High-Field Diffractometer at UE46 PGM-1.

References

Bernien, M., Naggert, H., Arruda, L. M., Kipgen, L., Nickel, F., Miguel, J., … Kuch, W. (2015). Highly Efficient Thermal and Light-Induced Spin-State Switching of an Fe(II) Complex in Direct Contact with a Solid Surface. *ACS Nano*, *9*(9), 8960-8966. http://dx.doi.org/10.1021/acsnano.5b02840

Blanco-Canosa, S., Frano, A., Loew, T., Lu, Y., Porras, J., Ghiringhelli, G., … Keimer, B. (2013). Momentum-Dependent Charge Correlations in $YBa_2Cu_3O_{6+\delta}$ Superconductors Probed by Resonant X-Ray Scattering: Evidence for Three Competing Phases. *Phys. Rev. Lett.*, *110*, 187001. http://dx.doi.org/10.1103/PhysRevLett.110.187001

Comin, R., Frano, A., Yee, M. M., Yoshida, Y., Eisaki, H., Schierle, E., … Damascelli, A. (2014). Charge Order Driven by Fermi-Arc Instability in $Bi_2Sr_{2-x}La_{2-x}Cu0_{6+\delta}$. *Science*, *343*(6169), 390-392. http://dx.doi.org/10.1126/science.1242996

da Silva Neto, E. H., Aynajian, P., Frano, A., Comin, R., Schierle, E., Weschke, E., … Yazdani, A. (2014). Ubiquitous Interplay Between Charge Ordering and High-Temperature Superconductivity in Cuprates. *Science*, *343*(6169), 393–396. http://dx.doi.org/10.1126/science.1243479

Englisch, U., Rossner, H., Maletta, H., Bahrdt, J., Sasaki, S., Senf, F., … Gudat, W. (2001). The elliptical undulator UE46 and its monochromator beam-line for structural research on nanomagnets at BESSY-II. *Nuclear Instruments and Methods in Physics Research Section A: Accelerators, Spectrometers, Detectors and Associated Equipment*, *467-468*(Part 1), 541 - 544. http://dx.doi.org/10.1016/S0168-9002(01)00407-7

Fink, J., Schierle, E., Weschke, E., & Geck, J. (2013). Resonant elastic soft x-ray scattering. *Reports on Progress in Physics*, *76*(5), 056502. http://dx.doi.org/10.1088/0034-4885/76/5/056502

Fink, J., Schierle, E., Weschke, E., Geck, J., Hawthorn, D., Soltwisch, V., … Sawatzky, G. A. (2009). Charge ordering in $La_{1.8-x}Eu_{0.2}Sr_xCuO_4$ studied by resonant soft x-ray diffraction. *Phys. Rev. B*, *79*, 100502. http://dx.doi.org/10.1103/PhysRevB.79.100502

Follath, R., & Senf, F. (1997). New plane-grating monochromators for third generation synchrotron radiation light sources. *Nuclear Instruments and Methods in Physics Research Section A: Accelerators, Spectrometers, Detectors and Associated Equipment*, *390*(3), 388 - 394. http://dx.doi.org/10.1016/S0168-9002(97)00401-4

Frano, A., Schierle, E., Haverkort, M. W., Lu, Y., Wu, M., Blanco-Canosa, S., … Keimer, B. (2013). Orbital Control of Noncollinear Magnetic Order in Nickel Oxide Heterostructures. *Phys. Rev. Lett.*, *111*, 106804. http://dx.doi.org/10.1103/PhysRevLett.111.106804

Ghiringhelli, G., Le Tacon, M., Minola, M., Blanco-Canosa, S., Mazzoli, C., Brookes, N. B., … Braicovich, L. (2012). Long-Range Incommensurate Charge Fluctuations in $(Y,Nd)Ba_2Cu_3O_{6+x}$. *Science*, *337*(6096), 821–825. http://dx.doi.org/10.1126/science.1223532

Glavic, A., Becher, C., Voigt, J., Schierle, E., Weschke, E., Fiebig, M., & Brückel, T. (2013). Publisher's Note: Stability of spin-driven ferroelectricity in the thin-film limit: Coupling of magnetic and electric order in multiferroic $TbMnO_3$ films [Phys. Rev. B 88, 054401 (2013)]. *Phys. Rev. B*, *88*, 059904. http://dx.doi.org/10.1103/PhysRevB.88.059904

Graf, C., Goroncy, C., Stumpf, P., Weschke, E., Boeglin, C., Ronneburg, H., & Rühl, E. (2015). Local Magnetic and Electronic Structure of the Surface Region of Postsynthesis Oxidized Iron Oxide Nanoparticles for Magnetic Resonance Imaging. *The Journal of Physical Chemistry C*, *119*(33), 19404-19414. http://dx.doi.org/10.1021/jp512023z

Hermanns, C. F., Bernien, M., Krüger, A., Schmidt, C., Waßerroth, S. T., Ahmadi, G., … Kuch, W. (2013). Magnetic Coupling of $Gd_3\mathbf{N}@\mathbf{C}_{80}$ Endohedral Fullerenes to a Substrate. *Phys. Rev. Lett.*, *111*, 167203. http://dx.doi.org/10.1103/PhysRevLett.111.167203

Khalid, M., Weschke, E., Skorupa, W., Helm, M., & Zhou, S. (2014). Ferromagnetism and impurity band in a magnetic semiconductor: InMnP. *Phys. Rev. B*, *89*, 121301. http://dx.doi.org/10.1103/PhysRevB.89.121301

Leininger, P., Ilakovac, V., Joly, Y., Schierle, E., Weschke, E., Bunau, O., … Foury-Leylekian, P. (2011). Ground State of the Quasi-1D Compound $BaVS_3$ Resolved by Resonant Magnetic X-Ray Scattering. *Phys. Rev. Lett.*, *106*, 167203. http://dx.doi.org/10.1103/PhysRevLett.106.167203

Leininger, P., Rahlenbeck, M., Raichle, M., Bohnenbuck, B., Maljuk, A., Lin, C. T., … Freeland, J. W. (2010). Electronic structure, magnetic, and dielectric properties of the edge-sharing copper oxide chain compound $NaCu_2O_2$. *Phys. Rev. B*, *81*, 085111. http://dx.doi.org/10.1103/PhysRevB.81.085111

Matsuda, T., Partzsch, S., Tsuyama, T., Schierle, E., Weschke, E., Geck, J., … Wadati, H. (2015). Observation of a Devil's Staircase in the Novel Spin-Valve System $SrCo_6O_{11}$. *Phys. Rev. Lett.*, *114*, 236403. http://dx.doi.org/10.1103/PhysRevLett.114.236403

Partzsch, S., Wilkins, S. B., Hill, J. P., Schierle, E., Weschke, E., Souptel, D., … Geck, J. (2011). Observation of Electronic Ferroelectric Polarization in Multiferroic YMn_2O_5. *Phys. Rev. Lett.*, *107*, 057201. http://dx.doi.org/10.1103/PhysRevLett.107.057201

Princep, A. J., Mulders, A. M., Schierle, E., Weschke, E., Hester, J., Hutchison, W. D., … Nakamura, T. (2012). High-order Ho multipoles in $HoB_2\ C_2$ observed with soft resonant x-ray diffraction. *Journal of Physics: Condensed Matter*, *24*(7), 075602. http://dx.doi.org/10.1088/0953-8984/24/7/075602

Radu, F., Abrudan, R., Radu, I., Schmitz, D., & Zabel, H. (2012). Perpendicular exchange bias in ferrimagnetic spin valves. *Nature Communications*, *3*, 715. http://dx.doi.org/10.1038/ncomms1728

Schierle, E., Soltwisch, V., Schmitz, D., Feyerherm, R., Maljuk, A., Yokaichiya, F., … Weschke, E. (2010). Cycloidal Order of $4f$ Moments as a Probe of Chiral Domains in $DyMnO_3$. *Phys. Rev. Lett.*, *105*, 167207. http://dx.doi.org/10.1103/PhysRevLett.105.167207

Schmitz, D., Schmitz-Antoniak, C., Warland, A., Darbandi, M., Haldar, S., Bhandary, S., … Wende, H. (2014). The dipole moment of the spin density as a local indicator for phase transitions. *Scientific Reports*, *4*, 5760. http://dx.doi.org/10.1038/srep05760

Schmitz-Antoniak, C., Schmitz, D., Borisov, P., de Groot, F. M. F., Stienen, s., Warland, A., … Wende, H. (2013). Electric in-plane polarization in multiferroic $CoFe_2O_4/BaTiO_3$ nanocomposite tuned by magnetic fields. *Nature Communications*, *4*, 2051. http://dx.doi.org/10.1038/ncomms3051

Shiozawa, H., Briones-Leon, A., Domanov, O., Zechner, G., Sato, Y., Suenaga, K., … Pichler, T. (2015). Nickel clusters embedded in carbon nanotubes as high performance magnets. *Scientific Reports*, *5*, 15033. http://dx.doi.org/10.1038/srep15033

Skaugen, A., Schierle, E., van der Laan, G., Shukla, D. K., Walker, H. C., Weschke, E., & Strempfer, J. (2015). Long-range antiferromagnetic order of formally nonmagnetic Eu^{3+} Van Vleck ions observed in multiferroic $Eu_{1-x}Y_xMnO_3$. *Phys. Rev. B*, *91*, 180409. http://dx.doi.org/10.1103/PhysRevB.91.180409

Strigari, F., Willers, T., Muro, Y., Yutani, K., Takabatake, T., Hu, Z., … Severing, A. (2013). Crystal field ground state of the orthorhombic Kondo semiconductors $CeOs_2Al_{10}$ and $CeFe_2Al_{10}$. *Phys. Rev. B*, *87*, 125119. http://dx.doi.org/10.1103/PhysRevB.87.125119

Wadati, H., Hawthorn, D. G., Geck, J., Higuchi, T., Hikita, Y., Hwang, H. Y., … Sawatzky, G. A. (2009). Resonant soft x-ray scattering studies of interface reconstructions in $SrTiO_3/LaAlO_3$ superlattices. *Journal of Applied Physics*, *106*(8), 083705. http://dx.doi.org/10.1063/1.3246788

Willers, T., Adroja, D. T., Rainford, B. D., Hu, Z., Hollmann, N., Körner, P. O., … Severing, A. (2012). Spectroscopic determination of crystal-field levels in $CeRh_2Si_2$ and $CeRu_2Si_2$ and of the $4f^0$ contributions in CeM_2Si_2 (M=Cu, Ru, Rh, Pd, and Au). *Phys. Rev. B*, *85*, 035117. http://dx.doi.org/10.1103/PhysRevB.85.035117

Willers, T., Cezar, J. C., Brookes, N. B., Hu, Z., Strigari, F., Körner, P., … Severing, A. (2011). Magnetic Field Induced Orbital Polarization in Cubic $YbInNi_4$: Determining the Quartet Ground State Using X-Ray Linear Dichroism. *Phys. Rev. Lett.*, *107*, 236402. http://dx.doi.org/10.1103/PhysRevLett.107.236402